Integrin Ligands (1)

International Edition: DOI: 10.1002/anie.201508709
German Edition: DOI: 10.1002/ange.201508709

Stable Peptides Instead of Stapled Peptides: Highly Potent αvβ6-Selective Integrin Ligands

*Oleg V. Maltsev, Udaya Kiran Marelli, Tobias G. Kapp, Francesco Saverio Di Leva, Salvatore Di Maro, Markus Nieberler, Ute Reuning, Markus Schwaiger, Ettore Novellino, Luciana Marinelli, and Horst Kessler**

Abstract: *The αvβ6 integrin binds the RGD-containing peptide of the foot and mouth disease virus with high selectivity. In this study, the long binding helix of this ligand was downsized to an enzymatically stable cyclic peptide endowed with sub-nanomolar binding affinity toward the αvβ6 receptor and remarkable selectivity against other integrins. Computational studies were performed to disclose the molecular bases underlying the high binding affinity and receptor subtype selectivity of this peptide. Finally, the utility of the ligand for use in biomedical studies was also demonstrated here.*

Helices are common binding motifs in protein–protein interactions.[1] However, the helix motifs in peptides are rarely used in medicinal chemistry because of their structural and enzymatic instability. A common approach used to overcome this problem is helix stabilization via "side-chain-to-side-chain" cyclization (so-called "stapled peptides").[2] In addition, side-on binding of helices can also be mimicked by β-sheet cyclic peptides, as demonstrated in the pioneering work of Robinson et al. (Figure 1).[3]

The integrin receptor family comprises at least 24 members, which are responsible for cell–cell and cell–extracellular matrix (ECM) interactions and adhesion processes.[4] Among these members, eight (αvβ1, αvβ3, αvβ5, αvβ6, αvβ8, αIIbβ3, α5β1, and α8β1) recognize the tripeptide Arg-Gly-Asp (RGD) motif in their ECM ligands. Compounds that are endowed with high binding affinity and selectivity toward a unique integrin subtype are the key pharmacological tools for an unambiguous understanding of the precise biological functions and cross-talk among different integrins. This knowledge, in turn, is the basis for personalized medicine. Although valuable inhibitors of αIIbβ3, αvβ3, and α5β1[5] have already been successfully developed, selective and active ligands are still absent for many other RGD-binding integrins.[6]

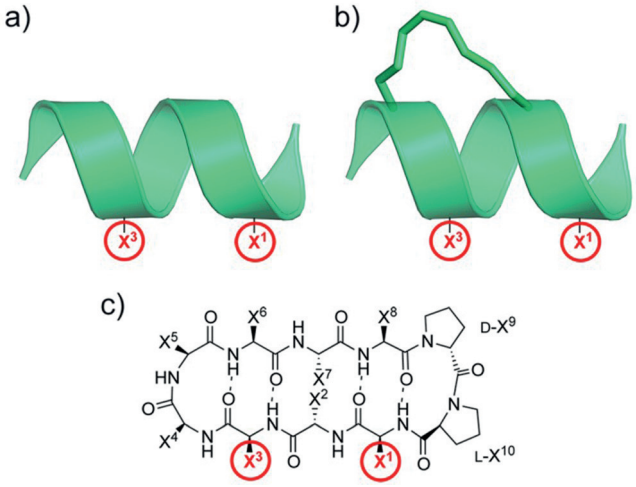

Figure 1. a) α-Helix with amino acids X^1 and X^3 responsible for protein–protein interactions. The helix is b) stabilized via "side-chain-to-side-chain" cyclization, and c) mimicked by a β-sheet cyclic peptide.

Recently, attention has been drawn to αvβ6 integrin because it is a high-affinity receptor for many viruses, including foot and mouth disease,[7] and is overexpressed in multiple cancers[8] and fibrosis.[9] To date, only a limited number of αvβ6-integrin tracers for cancer diagnosis have been developed; these include linear 10- to 20-mer[10] and "stapled" cystine peptides.[11] The design of αvβ6-specific ligands began with the phage display-derived sequence RXDLXXL, which has been assumed to bind as a helix motif.[12]

In the present study, the pharmacophoric amino acids from the αvβ6 binding helix were grafted onto a β-sheet (Figure 1 c), a secondary structure frequently found at natural protein–protein interfaces and then cyclized using β-turn

[*] Dr. O. V. Maltsev, Dr. U. K. Marelli, T. G. Kapp, Prof. Dr. H. Kessler
Institute for Advanced Study and Center for Integrated Protein Science (CIPSM), Technische Universität München
Lichtenbergstrasse 4, 85747 Garching (Germany)
E-mail: kessler@tum.de

Dr. F. S. Di Leva, Prof. Dr. E. Novellino, Prof. Dr. L. Marinelli
Dipartimento di Farmacia, Università di Napoli Federico II
Via D. Montesano 49, 80131 Napoli (Italy)

Dr. S. Di Maro
DiSTABiF, Secondo Università di Napoli
Via Vivaldi 43, 81100 Caserta (Italy)

Dr. M. Nieberler
Department of Oral and Maxillofacial Surgery, University Hospital rechts der Isar, Technische Universität München
Ismaninger Strasse 22, 81675 München (Germany)

Prof. Dr. U. Reuning
Klinische Forschergruppe der Frauenklinik, University Hospital rechts der Isar, Technische Universität München
Ismaninger Strasse 22, 81675 München (Germany)

Prof. Dr. M. Schwaiger
Department of Nuclear Medicine, University Hospital rechts der Isar, Technische Universität München
Ismaninger Strasse 22, 81675 München (Germany)

Supporting information for this article is available on the WWW under http://dx.doi.org/10.1002/anie.201508709.

mimics. Subsequently, a library of enzymatically stable cyclic peptides was generated from the switching and modification of the amino acids. Binding affinity/selectivity studies of the peptides library led to the discovery of a novel ligand for αvβ6 integrin, which has the lowest molecular weight of all αvβ6 ligands identified to date. Notably, this ligand is endowed with sub-nanomolar binding affinity and remarkable selectivity for the αvβ6 integrin subtype.

As a starting point, we used the cyclic decapeptides first described by Robinson et al.,[3] i.e., those bearing the D-Pro-L-Pro (pP) β-hairpin-inducing template, which were shown to be structurally tolerant to the amino acid changes at other positions of the β-sheet-like structure. Because the optimal location of the RGDL or RTDL motif was not known a priori, we decided to check all the putative positions of this motif along the macrocycle. The position of the second leucine in the DLXXL sequence was variable and in some cases interrupted by the introduction of a pP hairpin-inducing unit. Other amino acid residues were replaced with L-alanines to explore the importance of the amino acids' side chains. We planned to optimize the chemical structures of these amino acids in a later step.

As a result of the aforementioned process, 10 novel cyclic peptides containing RGD (Table 1) or RTD (see the Supporting Information, SI) were designed and synthesized using Fmoc solid-phase peptide synthesis (SPPS) and cyclization in solution.[13] In all cases, RTD-bearing peptides displayed lower (5- to 107-fold) αvβ6 binding affinities than the respective RGD-containing versions (see SI). Impressively, the first three synthesized RGD peptides **1**–**3** (Table 1) were able to bind to the αvβ6 integrin receptor in a low nanomolar range (5.8 to 14.5 nM), which indicated the power of the strategy used. Despite its relatively high αvβ3 binding affinity (76.7 nM), peptide **2**, which had the highest αvβ6 binding affinity, was chosen as a new lead structure.

Table 1: Binding affinities of compounds **1**–**10** for αvβ6 and αvβ3 as determined in a solid-phase binding assay using a previously established protocol.[14]

Peptide	Amino acid sequence (X^1–X^{10})	αvβ6, IC_{50} [nM]	αvβ3, IC_{50} [nM]
1	**RGD**LAALApP	14.5	–
2	A**RGD**LAALpP	8.3	76.7
3	LA**RGD**LAApP	13.4	–
4	A**RGD**AAALpP	320	–
5	A**RGD**LAAApP	15.4	–
6	A**RGD**LA-LpP	3.0	106
7	A**RGD**LA-FpP	0.67	104
8	F**RGD**LA-LpP	1.25	>1000
9	F**RGD**LA-Fp(*N*Me)K	0.26	632
10	F**RGD**LA-Fp(*N*Me)K(Ac)	0.30	640

Surprisingly, in contrast to the situation in linear peptides, the DLXXL motif was not essential for the αvβ6 activity of our cyclic peptides.[10–12] Indeed, in peptide **3** the pP β-turn-inducing moiety was introduced to break the DLXXL, and this caused no drastic change in αvβ6 binding affinity. To better clarify the importance of the LXXL motif in αvβ6 binding, we replaced the Leu residues at positions 5 and 8 with L-Ala (**2** in Table 1). Intriguingly, the presence of Leu next to RGD (peptide **4**) was crucial for αvβ6 recognition, whereas a substitution of the second Leu (peptide **5**) led to only a slight drop in binding affinity, which was in line with the binding affinity of **3**. Given this observation, we assumed that deletion of one or several amino acids from the macrocycle might be possible with the aim of further simplifying the ligand structure. Indeed, the removal of one Ala residue (peptide **6**) led to an αvβ6 ligand with the same binding affinity but reduced αvβ3 binding affinity (see SI). Further removal of amino acids was inefficient and drastically lowered the αvβ6 binding affinity (see SI).

Following a few unsuccessful attempts to improve ligand αvβ6 binding affinity and selectivity via adjustment of amino acid X^6 (see SI), we postulated that this structural fragment must be kept as small (i.e. alanine) as in previously reported linear peptides, e.g., H2009.1, RGDLATLRQL, and *c*(-CRGDLASLC-).[10–12]

The RGD flanking Leu appeared to be essential in the nonapeptides, as in 10-mer peptides (see SI). Furthermore, the second Leu could be easily replaced by other bulky amino acids with a positive effect on binding affinity. Thus, the Leu→Phe substitution led to a fivefold enhancement of binding affinity toward αvβ6 integrin without any noticeable impact on αvβ3 binding affinity (peptide **7**). Remarkably, the substitution of RGD flanking L-Ala with the sterically demanding L-Phe (peptide **8**) resulted in a considerable loss of binding affinity for αvβ3 together with a slight improvement in αvβ6 binding affinity. Similarly, L-Thr and L-Trp at positions X^1 and X^8 also improved the ligand binding properties; however, these improvements were inferior to that observed with L-Phe (see SI).

Once the locations and nature of the key amino acids were established, we decided to optimize the X^9–X^{10} residues to ensure they were suitable for functionalization of the compound for applications such as molecular imaging and surface coating.[15] *N*-Methylation is a well-known strategy for creating proline mimetics as well as a tool for improving the properties of peptides, including stability, affinity, and bioavailability.[16] Here, we substituted one of the prolines with a *N*Me lysine whose side chain offered opportunities for further functionalization. Interestingly, we found that only L-Pro^{10} could be efficiently replaced with *N*Me-L-Lys, whereas changing D-Pro^9 into the respective *N*Me-D-Lys reduced both binding affinity and subtype selectivity (see SI). Furthermore, the NH_2 group on the lysine side chain apparently did not contribute to receptor binding because its acetylation did not influence the IC_{50} of **10**.

We also investigated a wider selectivity profile of the most active peptides, **9** and **10**. Our assays revealed that both peptides possessed low binding affinity toward αIIbβ3, αvβ3, and αvβ5, but a residual binding affinity for α5β1 and αvβ8 integrins. However, as shown in Table 2, the affinity of **9** and **10** toward αvβ6 was always at least two orders of magnitude higher than that of other RGD binding integrins. Thus, to the best of our knowledge, **9** and **10** are currently the most potent and selective cyclic peptides toward αvβ6 integrin described in the literature.[17] For reducing the residual binding affinity

Table 2: Binding affinities of cyclic peptides **9** and **10** toward αvβ6, αvβ3, α5β1, αvβ8, αIIbβ3, and αvβ5 integrins, and their selectivities for αvβ6, determined in a solid-phase binding assay using a previously established protocol.[14]

Peptide	αvβ6, IC_{50} [nM]	αvβ3, IC_{50} [nM]	α5β1, IC_{50} [nM]	αvβ8, IC_{50} [nM]	αIIbβ3, IC_{50} [nM]	αvβ5, IC_{50} [nM]
9	0.26	632 1:2431	72.9 1:280	23.6 1:91	>1000 –	>1000 –
10	0.30	640 1:2133	74.0 1:247	21.1 1:70	>1000 –	>1000 –

for α5β1, a new approach, including the incorporation of an *N*-alkylated arginine guanidine group was followed and yielded an arginine N_{ω}Et derivative of **10**. This compound possesses the same binding affinity for αvβ6 (0.28 nM) while being inactive towards α5β1 (>10 μM).[18]

To reveal the molecular basis of the peptide binding properties, we assessed the solution conformation of **10**[19] using NMR spectroscopy. A single set of ^{1}H chemical shifts was observed, which indicated a predominant conformation on the NMR timescale. The NMR data suggested that peptide **10** assumes an antiparallel β-sheet structure (Figure 2). Thus,

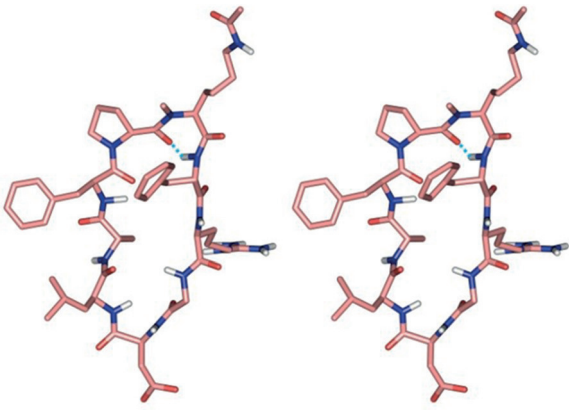

Figure 2. Stereoview of the NMR-derived conformation of peptide **10**. Nonpolar hydrogens have been omitted for clarity; hydrogen bonds are shown as light blue dotted lines.

the D-Pro^8-*N*Me-L-Lys^9 moiety acts as an analogue of the βII′-turn-inducing D-Pro-L-Pro template; however, in this case, there was a clearly evident inverse γ-turn centered at L-*N*Me-Lys^9(Ac) with dihedral angles of $\phi = -82.4°$ and $\psi = 52.6°$ and a hydrogen bond between Phe^1-NH and D-Pro^8-CO.[20] The dihedral angles $\phi = 56.2°$ and $\psi = -178.3°$ for D-Pro^8, when combined with those for L-*N*Me-Lys^9(Ac), support a distorted βII′ turn around the D-Pro^8-L-*N*Me-Lys^9(Ac), which is consistent with the equilibrium of a γ turn with a βII′ turn. The structure revealed that the lipophilic chains of Phe^1, Leu^5, and Phe^7 are oriented to the same side of the plane of the cycle, whereas RGD points in the opposite direction (Figure 2).

The NMR structure of **10** was then used to investigate the peptide binding mode at the αvβ6 integrin by computational studies. Here, standard docking methods were not feasible since they cannot thoroughly sample the large conformational space of small to medium-sized peptides like **10** upon binding. For this reason, a manual docking of the averaged NMR structure of **10** in the αvβ6 crystal structure[21] (PDB code: 4UM9) was performed; this was followed by a 100 ns MD simulation of the resulting complex (see SI). Briefly, at the beginning of the MD simulation, **10** slightly rearranged its position and conformation (Figure 3), which was then con-

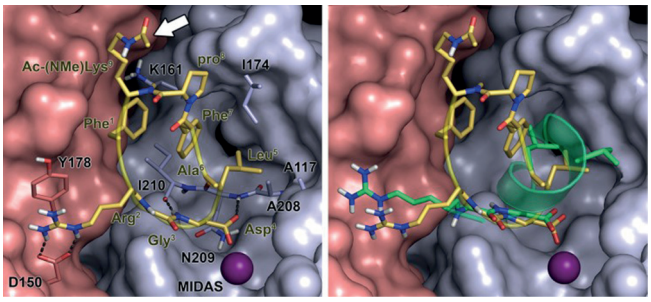

Figure 3. Binding mode of peptide **10** obtained through MD simulations (left) and superposition of peptide **10** and TGF-β3 at the αvβ6 integrin (right). Peptide **10** (yellow) and TGF-β3 (green) are shown as ribbons and sticks. The αvβ6 and β6 subunits are represented as light red and blue surfaces, respectively. The metal ion at the MIDAS is depicted as a purple sphere. Receptor amino acids important for peptide binding are highlighted as sticks. The αvβ6 crystal structure employed in the MD simulations was obtained from the protein databank (PDB code: 4UM9). In (a) the white arrow indicates the position of the functionalization with the fluorescence label.

served for the remainder of the simulation (see SI). Interestingly, the MD-generated binding mode was highly superimposable with that of the turn-helix motif of the transforming growth factor β3 (TGF-β3), which is co-crystallized with αvβ6 (Figure 3). Besides the well-known interactions of the RGD motif with the surface of integrins, the Leu^5 and Phe^7 side chains of **10** fit well into the wide lipophilic pocket located below the specificity-determining loop (SDL) in the β subunit,[21] interacting with (β6)-A117, (β6)-I174, and (β6)-A208, and with (β6)-I174 and (β6)-I210, respectively. We note that tight intramolecular hydrophobic packing involving the Phe^1, Leu^5, and Phe^7 side chains stabilized this interaction pattern. Indeed, the side chains all project in the same direction as the i, $i+4$, and $i+7$ residues in an α-helical motif similar to that of TGF-β3. These outcomes explain why the replacement of any of the latter three hydrophobic residues decreases the peptide affinity toward αvβ6 (**9**–**10** vs. **6**–**8**). Finally, according to the MD results, no specific interaction is formed by Ala^5, D-Pro^8, or (*N*Me)Lys(Ac)^9 of **10**, which suggests that these residues might play a structural role (i.e., stabilizing the peptide bioactive conformation) rather than being directly involved in the binding to αvβ6. Interestingly, the (*N*Me)Lys(Ac)^9 side chain points toward the solvent; this explains why the acylation of (*N*Me)Lys^9 does not significantly influence the peptide's affinity toward αvβ6. The binding mode predicted for **10** at the αvβ6 integrin can also help us to rationalize the molecular basis of its selectivity against the other tested integrins, particularly αvβ3 and α5β1. For instance, in αvβ3, the residues (β6)-A117, (β6)-K161,

(β6)-A208, and (β6)-I210 are replaced by the bulkier residues (β3)-Y122, (β3)-Y166, (β3)-R214, and (β3)-R216, respectively.[17a] These residues generate large steric hindrance, probably preventing the peptide Leu^5 and Phe^7 side chains from occupying the SDL region in αvβ3. This might in turn weaken the binding of the peptide RGD motif, which could explain why **10** binds this receptor with only a micromolar affinity. In α5β1, the aforementioned αvβ6 residues are instead replaced by (β1)-Y127, (β1)-S171, (β1)-G217, and (β1)-L219, respectively.[22] Among these replacements, only (β1)-Y127 and (β1)-L219 can establish favorable lipophilic interactions with the peptide Leu^5 and Phe^7 side chains, whereas the substitution of the hydrophobic (β6)-I174 with the polar (β1)-E184 can further reduce the affinity of **10** toward α5β1 compared with its affinity toward αvβ6.

Considering that the biological application of peptides is often limited by their metabolic susceptibility, the stability of the developed cyclic nonapeptides was assessed in human blood plasma and compared with that of the linear nonapeptide RTDLDSLRT[12a] as a reference. In contrast to the linear reference peptide, which degrades within 30 min by more than 50% (see SI), the cyclic peptides **9** and **10** remained unaltered for at least 3 h (i.e., the maximal time of observation in this study).

To demonstrate the biological use of the novel αvβ6 integrin selective ligands, we connected peptide **9** with Cy5.5 fluorescent dye via the Lys^9 side chain. We chose the highly aggressive and invasive human oral squamous carcinoma HN cell line, which has a high level of αvβ6 expression, as a model.[23] The human ovarian cancer cell line OVMZ6, which has low expression of αvβ6 and high expression of αvβ3, was used as a control.[24] Incubation of HN cells with **9-Cy5.5** resulted in a strong and specific fluorescence signal, restricted to the cell membrane of αvβ6-expressing carcinoma cells. In contrast, the **9-Cy5.5** conjugate displayed no binding to OVMZ6 cells or keratinocytes. (Figure 4 and Figure S4).

In conclusion, in this study, the RGD flanking binding helix of the known αvβ6 ligands derived from FMDV was downsized to an enzymatically stable cyclic peptide endowed with sub-nanomolar binding affinity and remarkable selectivity against other integrins. Together with computational studies, the NMR structure of the peptide provides insights into the molecular basis of its selectivity and binding affinity profile. Preliminary bioimaging studies on a human oral squamous carcinoma cell line strongly suggest feasible future applications for the peptide in medicine (e.g. for cancer diagnosis or therapy).

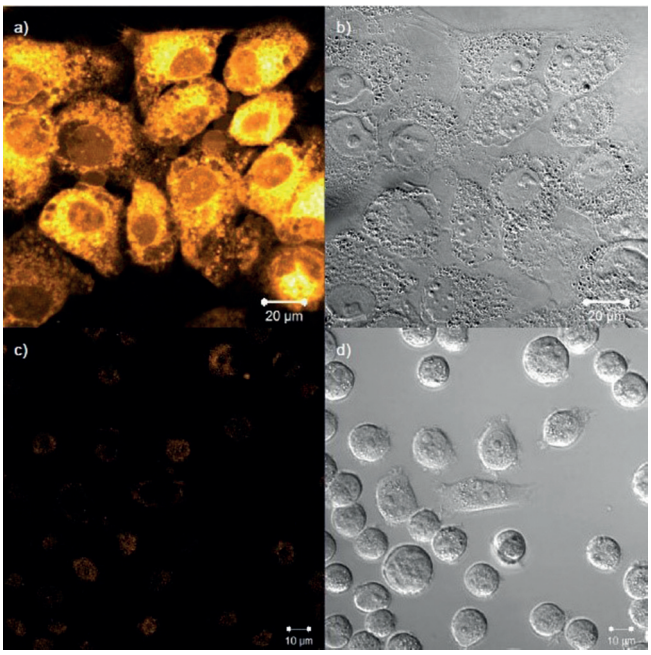

Figure 4. a) Fluorescence bioimaging of the human oral squamous cell carcinoma (OSCC) cell line HN, which has a high level of αvβ6-integrin expression, by using the Cy5.5-labeled **9**. b) Image the HN cells from (a) by transmitted light microscopy. c) Fluorescence bioimaging of the human ovarian cancer cell line OVMZ6, which has low integrin αvβ6 and high integrin αvβ3 expression, by using Cy5.5-labeled **9**. d) Illustration of the OVMZ6 cells from (c)by transmitted light microscopy.

Acknowledgements

H.K. acknowledges the Reinhard Koselleck grant of the Deutsche Forschungsgemeinschaft (Ke 147/42-1).

Keywords: cyclic peptides · integrin inhibitors · molecular imaging · subtype selectivity · αvβ6 integrin

How to cite: *Angew. Chem. Int. Ed.* **2016**, *55*, 1535–1539
Angew. Chem. **2016**, *128*, 1559–1563

[1] V. Azzarito, K. Long, N. S. Murphy, A. J. Wilson, *Nat. Chem.* **2013**, *5*, 161–173.
[2] a) L. D. Walensky, G. H. Bird, *J. Med. Chem.* **2014**, *57*, 6275–6288; b) C. Yu, J. W. Taylor, *Bioorg. Med. Chem.* **1999**, *7*, 161–175; c) T. A. Hill, N. E. Shepherd, F. Diness, D. P. Fairlie, *Angew. Chem. Int. Ed.* **2014**, *53*, 13020–13041; *Angew. Chem.* **2014**, *126*, 13234–13257.
[3] a) R. Fasan, R. L. Dias, K. Moehle, O. Zerbe, J. W. Vrijbloed, D. Obrecht, J. A. Robinson, *Angew. Chem. Int. Ed.* **2004**, *43*, 2109–2112; *Angew. Chem.* **2004**, *116*, 2161–2164; b) R. Fasan, R. L. Dias, K. Moehle, O. Zerbe, D. Obrecht, P. R. Mittl, M. G. Grutter, J. A. Robinson, *ChemBioChem* **2006**, *7*, 515–526.
[4] Y. Takada, X. Ye, S. Simon, *Genome Biol.* **2007**, *8*, 215.
[5] a) S. Neubauer, F. Rechenmacher, A. J. Beer, F. Curnis, K. Pohle, C. D'Alessandria, H. J. Wester, U. Reuning, A. Corti, M. Schwaiger, H. Kessler, *Angew. Chem. Int. Ed.* **2013**, *52*, 11656–11659; *Angew. Chem.* **2013**, *125*, 11870–11873; b) S. Rahmouni, A. Lindner, F. Rechenmacher, S. Neubauer, T. R. Sobahi, H. Kessler, E. A. Cavalcanti-Adam, J. P. Spatz, *Adv. Mater.* **2013**, *25*, 5869–5874; c) D. Heckmann, A. Meyer, L. Marinelli, G. Zahn, R. Stragies, H. Kessler, *Angew. Chem. Int. Ed.* **2007**, *46*, 3571–3574; *Angew. Chem.* **2007**, *119*, 3641–3644; d) F. Rechenmacher, S. Neubauer, J. Polleux, C. Mas-Moruno, M. De Simone, E. A. Cavalcanti-Adam, J. P. Spatz, R. Fassler, H. Kessler, *Angew. Chem. Int. Ed.* **2013**, *52*, 1572–1575; *Angew. Chem.* **2013**, *125*, 1612–1616; e) S. L. Goodman, M. Picard, *Trends Pharmacol. Sci.* **2012**, *33*, 405–412.
[6] T. G. Kapp, F. Rechenmacher, T. R. Sobahi, H. Kessler, *Expert Opin. Ther. Pat.* **2013**, *23*, 1273–1295.
[7] Y. Zhang, Y. Sun, F. Yang, J. Guo, J. He, Q. Wu, W. Cao, L. Lv, H. Zheng, Z. Zhang, *Viruses* **2013**, *5*, 1114–1130.

[8] a) A. Bandyopadhyay, S. Raghavan, *Curr. Drug Targets* **2009**, *10*, 645 – 652; b) D. M. Ramos, D. Dang, S. Sadler, *Anticancer Res.* **2009**, *29*, 125 – 130.
[9] a) A. L. Tatler, G. Jenkins, *Proc. Am. Thorac. Soc.* **2012**, *9*, 130 – 136; b) S. K. Agarwal, *Front. Pharmacol.* **2014**, *5*, 131.
[10] For a better review see selected recent publications: 20-mer A20FMDV2: a) A. E. John, J. C. Luckett, A. L. Tatler, R. O. Awais, A. Desai, A. Hab-good, S. Ludbrook, A. D. Blanchard, A. C. Perkins, R. G. Jenkins, J. F. Marshall, *J. Nucl. Med.* **2013**, *54*, 2146 – 2152; b) M. Ueda, T. Fukushima, K. Ogawa, H. Kimura, M. Ono, T. Yamaguchi, Y. Ikehara, H. Saji, *Biochem. Biophys. Res. Commun.* **2014**, *445*, 661 – 666; 20-mer H2009.1: c) B. P. Gray, S. Li, K. C. Brown, *Bioconjugate Chem.* **2013**, *24*, 85 – 96; multimerized RGDLATLRQL: d) A. N. Singh, M. J. McGuire, S. Li, G. Hao, A. Kumar, X. Sun, K. C. Brown, *Theranostics* **2014**, *4*, 745 – 760.
[11] For a better review see selected recent publications: cystine peptides: a) X. Zhu, J. Li, Y. Hong, R. H. Kimura, X. Ma, H. Liu, C. Qin, X. Hu, T. R. Hayes, P. Benny, S. S. Gambhir, Z. Cheng, *Mol. Pharmaceutics* **2014**, *11*, 1208 – 1217; b) J. R. Hsiao, Y. Chang, Y. L. Chen, S. H. Hsieh, K. F. Hsu, C. F. Wang, S. T. Tsai, Y. T. Jin, *Head Neck* **2010**, *32*, 160 – 172.
[12] a) S. Kraft, B. Diefenbach, R. Mehta, A. Jonczyk, G. A. Luckenbach, S. L. Goodman, *J. Biol. Chem.* **1999**, *274*, 1979 – 1985; b) J. L. Wagstaff, S. Vallath, J. F. Marshall, R. A. Williamson, M. J. Howard, *Chem. Commun.* **2010**, *46*, 7533 – 7535; c) J. L. Wagstaff, M. L. Rowe, S.-J. Hsieh, D. DiCara, J. F. Marshall, R. A. Williamson, M. J. Howard, *RSC Adv.* **2012**, *2*, 11019 – 11028.
[13] J. Chatterjee, B. Laufer, H. Kessler, *Nat. Protoc.* **2012**, *7*, 432 – 444.
[14] A. O. Frank, E. Otto, C. Mas-Moruno, H. B. Schiller, L. Marinelli, S. Cosconati, A. Bochen, D. Vossmeyer, G. Zahn, R. Stragies, E. Novellino, H. Kessler, *Angew. Chem. Int. Ed.* **2010**, *49*, 9278 – 9281; *Angew. Chem.* **2010**, *122*, 9465 – 9468.
[15] U. Hersel, C. Dahmen, H. Kessler, *Biomaterials* **2003**, *24*, 4385 – 4415.
[16] a) J. Chatterjee, F. Rechenmacher, H. Kessler, *Angew. Chem. Int. Ed.* **2013**, *52*, 254 – 269; *Angew. Chem.* **2013**, *125*, 268 – 283; b) O. Ovadia, S. Greenberg, J. Chatterjee, B. Laufer, F. Opperer, H. Kessler, C. Gilon, A. Hoffman, *Mol. Pharmaceutics* **2011**, *8*, 479 – 487; c) J. Chatterjee, C. Gilon, A. Hoffman, H. Kessler, *Acc. Chem. Res.* **2008**, *41*, 1331 – 1342; d) E. Biron, J. Chatterjee, O. Ovadia, D. Langenegger, J. Brueggen, D. Hoyer, H. A. Schmid, R. Jelinek, C. Gilon, A. Hoffman, H. Kessler, *Angew. Chem. Int. Ed.* **2008**, *47*, 2595 – 2599; *Angew. Chem.* **2008**, *120*, 2633 – 2637; e) J. Chatterjee, O. Ovadia, G. Zahn, L. Marinelli, A. Hoffman, C. Gilon, H. Kessler, *J. Med. Chem.* **2007**, *50*, 5878 – 5881; f) B. Laufer, J. Chatterjee, A. O. Frank, H. Kessler, *J. Pept. Sci.* **2009**, *15*, 141 – 146.
[17] a) A. Bochen, U. K. Marelli, E. Otto, D. Pallarola, C. Mas-Moruno, F. S. Di Leva, H. Boehm, J. P. Spatz, E. Novellino, H. Kessler, L. Marinelli, *J. Med. Chem.* **2013**, *56*, 1509 – 1519; b) A. Jonczyk, B. Diefenbach, S. Goodman, U. Groth, G. Zischinsky, EP1196433, **2000**.
[18] T. G. Kapp, M. Fottner, O. V. Maltsev, H. Kessler, *Angew. Chem. Int. Ed.* **2015**, *54*, DOI: 10.1002/ange.201508713; *Angew. Chem.* **2015**, *127*, DOI: 10.1002/anie.201508713.
[19] We chose peptide **10** for modeling studies, since it is the closest analogue of functionalized peptides, where the appropriate functionalization was planned to be introduced via an amide bond to the lysine side-chain NH_2.
[20] C. M. Nair, M. Vijayan, Y. V. Venkatachalapathi, P. Balaram, *J. Chem. Soc. Chem. Commun.* **1979**, 1183 – 1184.
[21] X. Dong, N. E. Hudson, C. Lu, T. A. Springer, *Nat. Struct. Mol. Biol.* **2014**, *21*, 1091 – 1096.
[22] L. Marinelli, A. Meyer, D. Heckmann, A. Lavecchia, E. Novellino, H. Kessler, *J. Med. Chem.* **2005**, *48*, 4204 – 4207.
[23] H. Kawamata, K. Nakashiro, D. Uchida, K. Harada, H. Yoshida, M. Sato, *Int. J. Cancer* **1997**, *70*, 120 – 127.
[24] M. A. Müller, J. Opfer, L. Brunie, L. A. Volkhardt, E. K. Sinner, D. Boettiger, A. Bochen, H. Kessler, K. E. Gottschalk, U. Reuning, *J. Mol. Biol.* **2013**, *425*, 2988 – 3000.

Received: September 17, 2015
Revised: October 26, 2015
Published online: December 9, 2015

